MICROSCOPIC MODEL OF RADIATIVE CAPTURE REACTIONS WITH CLUSTER POLARIZABILITY. APPLICATION TO ^{7}Be AND ^{7}Li

A.V. NESTEROV, V.S. VASILEVSKY, T.P. KOVALENKO

Bogolyubov Institute for Theoretical Physics, Nat. Acad. of Sci. of Ukraine
(14b, Metrolohichna Str., Kyiv 03680, Ukraine; e-mail: nesterov@bitp.kiev.ua)

PACS 21.60Gx; 24.10Cn; 25.20.-x; 25.40Lw; 26.65.+t

We apply the microscopic three-cluster model developed by the authors to study effects of cluster polarization on the capture reactions $^3\mathrm{He}\,(\alpha,\gamma)^7\mathrm{Be}$, $^3\mathrm{H}\,(\alpha,\gamma)^7\mathrm{Li}$, $^6\mathrm{Li}\,(p,\gamma)^7\mathrm{Be}$ and $^6\mathrm{Li}\,(n,\gamma)^7\mathrm{Li}$. These reactions are of great importance for the astrophysical applications. Thus main attention is paid to the cross section (or the astrophysical S factor) of the reactions at low energies. We also study thoroughly the correlations between the astrophysical S factor of the reactions at zero energy and various quantities associated with the ground state of a compound nucleus.

Introduction

The aim of the paper is to study how strongly the cluster polarization affects the cross section or astrophysical S factor of the capture reactions $^3\mathrm{He}\,(\alpha,\gamma)^7\mathrm{Be}$, $^3\mathrm{H}\,(\alpha,\gamma)^7\mathrm{Li}$, $^6\mathrm{Li}\,(p,\gamma)^7\mathrm{Be}$ and $^6\mathrm{Li}\,(n,\gamma)^7\mathrm{Li}$ in ^{7}Be and ^{7}Li nuclei. This investigation is stimulated by two factors.

First, the radiative capture and photonuclear reactions are a source of interesting and valuable information about the dynamics and the structure of nuclear systems. This information is of great importance for fundamental and applied investigations. It is well known that the cross section of the radiative capture and photodisintegration reactions (within the standard approximations) are determined by the wave functions of bound and continuous spectrum states of a compound nucleus. Thus, these reactions are a good testing site for numerous microscopic and semimicroscopic models to check the quality of wave functions obtained within the models. Such a test verifies both the internal and asymptotic parts of wave functions. From the other hand, these reactions are a basic stage of processes running inside the Sun and other stars and in the Universe. Astrophysical aspects of the reactions under consideration (related, e.g., to the problem of solar neutrinos and the abundance of light elements in the Universe after the Big Bang) are thoroughly discussed in [1–5]. Thus, the theoretical analysis of reactions is of great importance for understanding and revealing the main factors, which have a great impact on the processes, and for the prediction of a behavior of the cross section of reactions in the energy ranges dominating in the Sun and the Universe. Numerous experiments have been performed [6–17] to determine the astrophysical S factor of the reactions at energies which are relevant to astrophysical applications. Moreover, huge theoretical efforts have been undertaken within microscopic and semimicroscopic methods (see, e.g., [18–29]) to analyze these reactions and to establish the general features or to reveal the main substantial factors.

Second, in our recent papers [30, 31], we formulated a microscopic three-cluster model which was specially designed to take the polarizability of interacting clusters into account. We called it the cluster polarization. It was shown that the polarization of nuclei ^{3}He(^{3}H) and ^{6}Li, which were considered as two-cluster systems ($^3\mathrm{He} = d+p$, $^3\mathrm{H} = d+n$, and $^6\mathrm{Li} = ^4\mathrm{He}+d$) plays an important role and affects, to a great extent, the position of bound and resonance states in ^{7}Be and ^{7}Li nuclei. It was demonstrated that the smaller the binding energy (with respect to the lowest two-body disintegration threshold) of an interacting cluster, the larger the polarizability of the cluster. We demonstrated that the cluster polarization increases the interaction between clusters and thus results in an increase of the binding energy for bound states and a substantial decrease of the energy and the width of resonance states.

Based on the arguments put forward above, we will study the capture reactions in ^{7}Be and ^{7}Li nuclei. The main attention will be given to the investigation of the polarizability of the clusters involved in these reactions. In our early papers [32–34], we demonstrated that the collective monopole and quadrupole polarizations have very large effects on the radiative capture and photodisintegration reactions. In the present paper, we consider a more important and prominent type of polarization [30, 31]. As in [30, 31], we will use the three-cluster con-

T a b l e 1. Correspondence between the Faddeev amplitudes and binary channels in ^{7}Bi and ^{7}Li

	^{7}Be		^{7}Li	
Amplitude	Binary channel	Two-cluster system	Binary channel	Two-cluster system
$f_1(\mathbf{x}_1, \mathbf{y}_1)$	$^4\mathrm{He} + {}^3\mathrm{He}$	$^3\mathrm{He} = d + p$	$^4\mathrm{He} + {}^3\mathrm{H}$	$^3\mathrm{H} = d + n$
$f_2(\mathbf{x}_2, \mathbf{y}_2)$	$^6\mathrm{Li} + p$	$^6\mathrm{Li} = {}^4\mathrm{He} + d$	$^6\mathrm{Li} + n$	$^6\mathrm{Li} = {}^4\mathrm{He} + d$
$f_3(\mathbf{x}_3, \mathbf{y}_3)$	$^5\mathrm{Li} + d$	$^5\mathrm{Li} = {}^4\mathrm{He} + p$	$^5\mathrm{He} + d$	$^5\mathrm{He} = {}^4\mathrm{He} + n$

figuration $^4\mathrm{He} + d + p$ ($^4\mathrm{He} + d + n$) to consider the binary channels $^4\mathrm{He} + {}^3\mathrm{He}$ and $^6\mathrm{Li} + p$ ($^4\mathrm{He} + {}^3\mathrm{H}$ and $^6\mathrm{Li} + n$) in ^{7}Be (^{7}Li). According to [30, 31], we consider the polarizability of clusters ^{6}Li and ^{3}He (^{3}H) which are represented by the two-cluster configurations $^4\mathrm{He} + d$ and $d + p$ ($d + n$), respectively. We assume that the polarizability of these clusters affects the cross section or the astrophysical S factor of the capture reactions at low energies.

The paper is organized in the following way. In Section 1, we briefly consider main ideas of the microscopic model designed to take the cluster polarization into account. Some basic formulae we use to calculated the capture reactions are discussed. In Section 2, we justify our choice of the input parameters and present the main results for bound and continuous spectrum states. The detailed analysis of the effects of cluster polarization on the astrophysical S factor of the capture reactions is carried out as well.

1. Model Formulation

We slightly modify the microscopic model whose details are presented in [30, 31]. The novelty of the present model is that we included a mixture of states with different total spins S and total orbital momenta L. In [30,31], we restricted ourselves with the total spin $S = 1/2$, and, thus, the total orbital momentum was a good quantum number. In the present paper, we involve states with the total spins $S = 1/2$ and $S = 3/2$. For instance, the ground state of ^{7}Be or ^{7}Li with the total angular momentum $J = 3/2$ will be characterized by the following combination: $(L, S) = (1, 1/2) + (1, 3/2)$. Note that the channels with the total spin $S = 3/2$ are realized when the spins of a deuteron and a proton (neutron) are aligned in the same direction. Thus, it is assumed within the model that there is no bound state in ^{3}He (^{3}H). In other words, this spin state gives no contribution to the bound state of ^{3}He (^{3}H).

A trial wave function reads

$$\Psi^J = \widehat{\mathcal{A}}\left\{\left[\Phi_1(A_1)\,\Phi_2(A_2)\,\Phi_3(A_3)\right]_S \times \right.$$

$$\left. \times \left[f_1(\mathbf{x}_1, \mathbf{y}_1) + f_2(\mathbf{x}_2, \mathbf{y}_2) + f_3(\mathbf{x}_3, \mathbf{y}_3)\right]_L\right\}_J, \qquad (1)$$

where $\Phi_\alpha(A_\alpha)$ is the shell-model wave function for the internal motion of cluster α ($\alpha = 1, 2, 3$), and $f_\alpha(\mathbf{x}_\alpha, \mathbf{y}_\alpha)$ is the Faddeev amplitude. In Table 1, we define all values related to Faddeev amplitudes. Note that the Jacobi vector $\mathbf{x}_\alpha$ connects the center of mass of clusters indicated in the column "Two-cluster system", while the Jacobi vector $\mathbf{y}_\alpha$ determines the distance between clusters indicated in the column "Binary channel". We underline that the binary channels mentioned in Table 1 are the dominant binary configurations in ^{7}Be and ^{7}Li. They are obtained by the projection of three-cluster configurations $^4\mathrm{He} + d + p$ and $^4\mathrm{He} + d + n$ onto the space of two-cluster configurations. This projection is a necessary step to incorporate the proper boundary conditions, which is of great importance for scattering states. Clusters indicated in the column "Two-cluster system" are a subject for the cluster polarization. They are represented as two-cluster subsystems.

We note that the wave function (1) is written within the LS coupling scheme, when the total spin S is a vector sum of spin individual clusters, the total orbital momentum L is a vector sum of partial orbital momenta, and the total angular momentum $\mathbf{J} = \mathbf{L} + \mathbf{S}$. This scheme can be used to calculate the spectrum of a three-cluster system. However, one has to use the JJ coupling scheme to study continuous-spectrum states.

To proceed further, we need to construct a wave function of two-cluster subsystems. We denote this function as $\Psi_\alpha^{J_\alpha}$ and represent it as

$$\Psi_\alpha^{J_\alpha} = \widehat{\mathcal{A}}_\alpha \left\{\left[\Phi_\beta(A_\beta)\,\Phi_\gamma(A_\gamma)\right]_{S_\alpha}\left[g_\alpha(\mathbf{x}_\alpha)\right]_{\lambda_\alpha}\right\}_{J_\alpha}, \qquad (2)$$

where $\widehat{\mathcal{A}}_\alpha$ is the antisymmetrization operator for the two-cluster system. This system consists of two clusters with numbers β and γ. (The indices α, β, and γ form a cyclic permutation of 1, 2, and 3). The function $\Psi_\alpha^{J_\alpha}$ has to be determined by solving the Schrödinger equation for a particular two-cluster subsystem. By solving this equation, we obtain the spectrum and the wave functions of bound states, as well as pseudobound states. These pseudobound states, being specific states of the two-cluster continuous spectrum, allow one to study the flexibility or polarizability of a two-cluster compound system.

In [30, 31], we made use of the Gaussian basis to expand the unknown function $g_\alpha(\mathbf{x}_\alpha)$ and to reduce the Schrödinger equation for a two-cluster subsystem to that of a simple matrix form, which can be easily solved numerically. The advantage of the Gaussian basis is that it allows one to describe the bound states of weakly bound nuclei with a minimal set of functions.

Let us enumerate the eigenstates of a two-cluster Hamiltonian by index σ. Thus, we have got the energy $E_\sigma^{(\alpha)}$and the wave functions $g_{\sigma\alpha}(\mathbf{x}_\alpha)$. Having got the set of two-cluster functions $g_{\sigma\alpha}(\mathbf{x}_\alpha)$, we can use them to expand the three-cluster function:

$$\Psi^J = \sum_\alpha \sum_\sigma \widehat{\mathcal{A}} \{[\Phi_1(A_1)\Phi_2(A_2)\Phi_3(A_3)]_S \times$$

$$\times [g_{\sigma\alpha}(\mathbf{x}_\alpha)\varphi_{\sigma\alpha}(\mathbf{y}_\alpha)]_L\}_J . \quad (3)$$

This is a typical and rather popular way to solve many-particle problems.

We now determine a set of wave functions $\varphi_{\sigma\alpha}(\mathbf{y}_\alpha)$ which characterize the relative motion of a cluster with the number α with respect to the center of mass of the two-cluster subsystem formed by clusters with numbers β and γ. The sum of the energy $\mathcal{E}_\alpha$ of internal motion of cluster α ($\mathcal{E}_\alpha$ is the eigenenergy of the single-cluster Hamiltonian) and the energy $E_\sigma^{(\alpha)}$ of the two-cluster system determines the energy of two-body threshold. Thus, by using expansion (3), we reduced our three-cluster system to the set of coupled multichannel two-body systems. In these three-cluster and two-body systems, the Pauli principle is treated in exact manner, and the interaction within each two-body system and the coupling of the channels are determined by a superposition of nucleon-nucleon potentials.

It should be noted that the present model provides a more advanced description of the internal structure of clusters, which are described by functions (3) and listed in Table 1 in the column "Two-cluster system". If we take only the function of a bound state(s) of the two-cluster subsystem, we have got rigid or nonflexible clusters. They don't change their shape and size, while interacting with the third cluster. If one or more wave functions of pseudobound states are involved, we have got a flexible cluster and thus all meanings to study the cluster polarization. In what follows, we will distinguish two cases. The first case corresponds to a rigid cluster, and it will be denoted as "N", which means that the polarization is not taken into account for a selected two-cluster subsystem. In this case, only one function $g_{\sigma\alpha}(\mathbf{x}_\alpha)$ with $\sigma = 0$ is involved in calculations. The second case denoted by "Y" takes the polarizability of the subsystem into account, so that all functions $g_{\sigma\alpha}(\mathbf{x}_\alpha)$ are involved in calculations.

To determine the energy and wave functions of bound states or the S-matrix and wave functions of continuous-spectrum states, we make use of the oscillator basis. It is incorporated to expand the functions $\varphi_{\sigma\alpha}(\mathbf{y}_\alpha)$ and to simplify the solution of the Schrödinger equation by reducing it to a system of linear equations. The main advantage of the oscillator basis is that it allows one to impose the proper boundary conditions for bound and scattering states (see details in [35–38]).

The cross section of radiative capture for an electric transition of polarity λ is

$$\sigma_{l_i J_i \to l_f J_f}^{E\lambda} = \frac{8\pi}{\hbar} \frac{k_\gamma^{2\lambda+1}}{(2S_1+1)(2S_2+1)} \frac{(\lambda+1)}{\lambda[(2\lambda+1)!!]^2} \times$$

$$\times \frac{(2J_f+1)}{(2l_i+1)} \sum_S \left| \left\langle \Psi_{l_f}^{J_f} \middle\| \widehat{M}_{E\lambda} \middle\| \Psi_{l_i S}^{J_i}(E) \right\rangle \right|^2 , \quad (4)$$

where S_1 and S_2 are the spins of incident clusters, J_i and J_f stand for the total angular momenta of incident and final states, respectively, and l_i and l_f denote the orbital momenta of the relative motion of two clusters in the initial and final states. Thus, to calculate the cross section or the astrophysical S factor, which is convenient to be used at astrophysical energies and related to the cross section by the relation

$$S(E) = \sigma(E) E \exp\{2\pi\eta\}$$

($\eta = Z_1 Z_2 e^2/\hbar v$ is the Sommerfeld parameter), we need to calculate the matrix element of the operator $\widehat{M}_{E\lambda}$ between the wave functions of the initial and final states. The electric λ-pole operator reads

$$\widehat{M}_{E\lambda} = e \sum_{i=1}^{A} \frac{1}{2}(1+\widehat{\tau}_{iz}) r_i^\lambda Y_{\lambda\mu}(\widehat{\mathbf{r}}_i) .$$

Here, $\mathbf{r}_i$ is a coordinate of the i-th nucleon in the center-of-mass system. In (4), it was assumed that the wave function of a bound state is normalized by the condition

$$\left\langle \Psi_{l_f}^{J_f} | \Psi_{l_f}^{J_f} \right\rangle = 1,$$

and the wave function of the continuous spectrum is of the unit flux

$$\Psi_{l_i S_i}^{J_i}(E) = \sqrt{\frac{\pi(2l_i+1)}{v}} \sum_{M_i} C_{l_i 0; S_i M_S}^{J_i M_i} \times$$

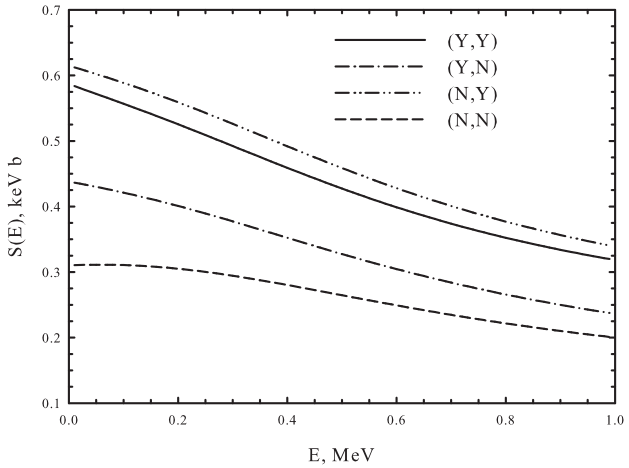

Fig. 1. Astrophysical factor for the reaction $^3\mathrm{He}\,(\alpha,\gamma)^7\mathrm{Be}$ with the cluster polarization effect

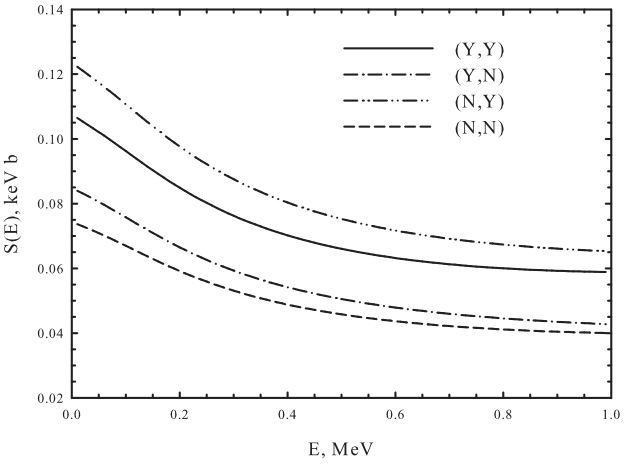

Fig. 2. Effects of cluster polarization on the S factor of the reaction $^3\mathrm{H}\,(\alpha,\gamma)^7\mathrm{Li}$

$$\times\widehat{\mathcal{A}}\left\{\left[\left[\Phi_1\left(A_1\right)\Phi_2\left(A_2\right)\right]^S Y_{l_i}\left(\widehat{\mathbf{y}}\right)\right]^{J_i M_i} g_{l_i J_i}\left(y\right)\right\}, \qquad (5)$$

where v is the relative velocity of two incident nuclei.

More details of calculations of the cross section of the radiative capture or photodisintegration can be found, for instance, in [20, 27, 28, 39].

In this paper, we consider only the electric dipole and quadrupole transitions, which dominate, as was shown repeatedly, in the low-energy region.

2. Results

To find the spectrum and the wave functions of discrete and continuous spectrum states of ^{7}Be and ^{7}Li, we employ the Minnesota potential (the central part is taken from [40] and the spin-orbital one is from [41] (set number IV)). In [30, 31], the parameter u of the potential was chosen to reproduce the experimental difference between the ^{4}He+^{3}He and $^6\mathrm{Li}+p$ (^{4}He+^{3}H and $^6\mathrm{Li}+n$) threshold energies. This was done in order to be consistent with the experimental situation for the reactions $^6\mathrm{Li}(p,^3\mathrm{He})^4\mathrm{He}$ and $^6\mathrm{Li}(n,^3\mathrm{H})^4\mathrm{He}$. Here, we use the same value of u. As in [30, 31], we chose the oscillator length, which is common for a deuteron and an alpha-particle, to minimize the energy of the three-cluster threshold $^4\mathrm{He}+d+p$ ($^4\mathrm{He}+d+n$).

We make use of 4 Gaussian functions and 130 oscillator functions to construct the wave functions of bound and continuous spectrum states of ^{7}Be and ^{7}Li. In [30,31] and in this paper, we made sure that this number of basis functions is large enough to provide the convergent solutions for scattering states and the cross section of nuclear rearrangement processes and radiative capture reactions. In what follows, we present four types of calculations, which will be distinguished by two letters: (N,N), (Y,N), (N,Y), and (Y,Y). The first letter indicates whether the polarization of ^{3}He(^{3}H) is regarded (Y) or disregarded (N) in calculations. The second letter is associated with the polarization of ^{6}Li cluster in the same way.

We start our calculations from the ground $J^\pi = 3/2^-$ states of ^{7}Be and ^{7}Li. Then we find their energy and wave function and calculate the quadrupole moment and the r.m.s. proton radius. We also determine the spectroscopic factor (SF) (see its definition, e.g., in [42]) for clusterizations 4+3 and 6+1. We obtain the energy and the wave function of the first excited $J^\pi = 1/2^-$ state and evaluate the $B\,(E2)$ transition probability from this state to the ground one. These quantities and the correlation between them will be discussed later at the end of this section. We now discuss the results of calculations of the S factor for the reactions $^3\mathrm{He}(\alpha,\gamma)^7\mathrm{Be}$, $^3\mathrm{H}\,(\alpha,\gamma)^7\mathrm{Li}$, $^6\mathrm{Li}\,(p,\gamma)^7\mathrm{Be}$ and $^6\mathrm{Li}\,(n,\gamma)^7\mathrm{Li}$.

In Fig. 1 (see also 2), we show the effects of cluster polarization on the S factor of the reactions $^3\mathrm{He}\,(\alpha,\gamma)^7\mathrm{Be}$ and $^3\mathrm{H}\,(\alpha,\gamma)^7\mathrm{Li}$ in the energy range $0 \le E \le 1$ MeV in the entrance channel. In these and other figures, we display only the dipole transition from the $1/2^+$ continuous-spectrum state to the ground state of a nucleus.

One immediately notices that the cluster polarization affects, to a great extent, the astrophysical S factor of the reactions $^3\mathrm{He}(\alpha,\gamma)^7\mathrm{Be}$ and $^3\mathrm{H}\,(\alpha,\gamma)^7\mathrm{Li}$. It changes the S factor at zero energy, as well as its dependence on the energy in the low-energy range. For both reactions,

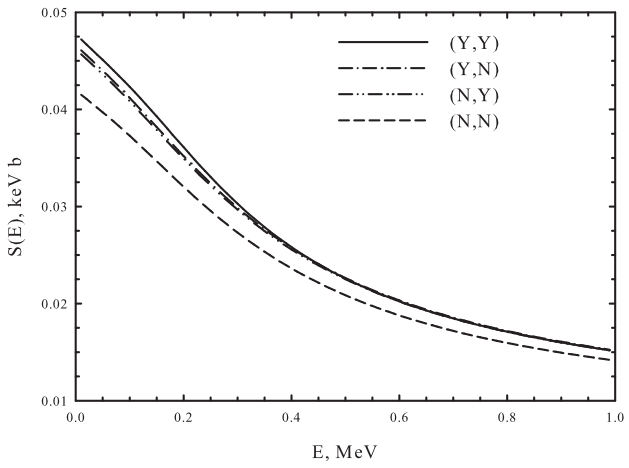

Fig. 3. Effects of the cluster polarization on the reaction $^6\mathrm{Li}\,(p,\gamma)^7\mathrm{Be}$

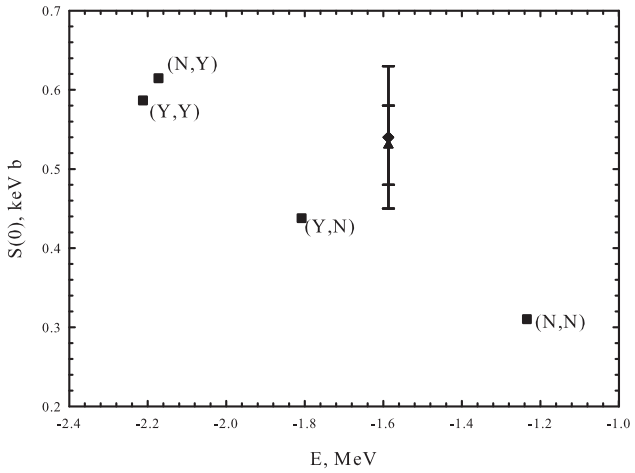

Fig. 4. Correlation between the astrophysical S factor of the reaction $^4\mathrm{He}\,(^3\mathrm{He},\gamma)^7\mathrm{Be}$ and the energy of the ^{7}Be ground state. Error bar marks the correlation between experimental values of the S factor and the energy of the ground state

the effect of the polarization of ^{6}Li is stronger than that for ^{3}He or ^{3}H.

Effects of the cluster polarization on the astrophysical S factor of the reaction $^6\mathrm{Li}\,(p,\gamma)^7\mathrm{Be}$ are shown in Fig. 3. One can see that the influence of the cluster polarization is not so strong as that for the reactions $^3\mathrm{He}\,(\alpha,\gamma)^7\mathrm{Be}$ and $^3\mathrm{H}\,(\alpha,\gamma)^7\mathrm{Li}$. In addition, effects of the cluster polarization on the reaction $^6\mathrm{Li}(n,\gamma)^7\mathrm{Li}$ are much more smaller than those for the reaction $^6\mathrm{Li}\,(p,\gamma)^7\mathrm{Be}$. We do not display a figure for this reaction. Note that a similar picture was observed in [30, 31] for the reactions $^6\mathrm{Li}(p,\alpha)^3\mathrm{He}$ and $^6\mathrm{Li}\,(n,\alpha)^3\mathrm{H}$: the cluster polarization affects stronger the cross section of the reaction $^6\mathrm{Li}\,(p,\alpha)^3$ He than that of the reaction $^6\mathrm{Li}\,(n,\alpha)^3\mathrm{H}$.

Tables 2 and 3 and Figs. 1–3 reveal nonlinear effects of the cluster polarization on the S factor of the capture reactions under investigations. The polarization of ^{6}Li and ^{3}He in cases (Y,N) and (N,Y) increases the value of S factor obtained without polarization (case (N,N)). With this result, one may expect that the higher the polarization, the larger the S factor of the capture reactions. However, if we involve both polarizations simultaneously (case (Y,Y)), then the S factor is decreased (one needs to compare it with that in case (N,Y)).

This conclusion is also confirmed by considering the dependence of the zero-energy S factor on parameters of the ground state. In Figs. 4–7, we demonstrate correlations between the zero-energy S factor ($S\,(0)$) and the energy (($E_{\mathrm{g.s.}}$)), r.m.s. proton radius (R_p), and quadrupole moment (Q) of the ground state. If we take three cases, namely (N,N), (Y,N), and (Y,Y), we observe simple, almost linear correlations between the $S\,(0)$

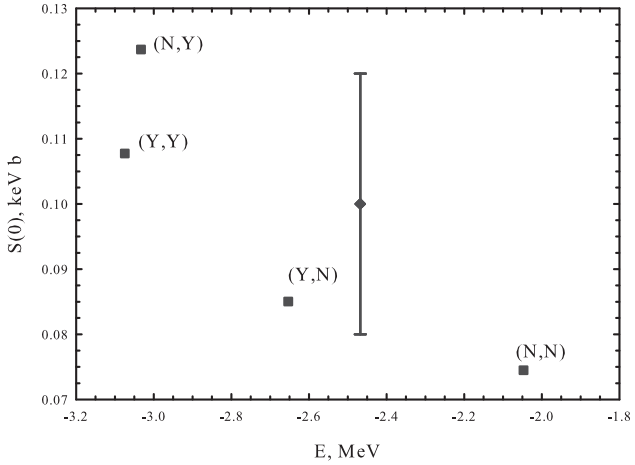

Fig. 5. Correlation between the astrophysical S factor of the reaction $^4\mathrm{He}\,(^3\mathrm{H},\gamma)^7\mathrm{Li}$ and the energy of the ^{7}Li ground state

factor and the energy $E_{\mathrm{g.s.}}$, radius R_p, and quadrupole moment Q of the ground state. The polarization of ^{6}Li taken alone into consideration violates such a simple correlation.

In Figs, 4–6, we display theoretical values of $S\,(0)$, $E_{\mathrm{g.s.}}$, and R_p and available experimental data. The ground-state energies of ^{7}Be and ^{7}Li nuclei are taken from [43]. The proton radius of ^{7}Be was determined in [44]. The analysis of experimental data carried out in [1] and [2] yielded two values for the S factor of the reaction $^3\mathrm{He}(\alpha,\gamma)^7\mathrm{Be}$, which are $S\,(0) = 0.54 \pm 0.09$ keV b and $S\,(0) = 0.53 \pm 0.05$ keV b, respectively. We use

T a b l e 2. Correlations between the astrophysical S factor $S(0)$ and the energy of the ^{7}Be ground state $E(\frac{3}{2}^-)$, quadrupole moment Q, r.m.s. proton radius R_p, and spectroscopic factor SF for the clusterization ^{4}He+^{3}He and ^{6}Li + p

Polarization		^{7}Be					
^{3}He	^{6}Li	$S(0)$, keV b	$E\left(\frac{3}{2}^-\right)$, MeV	Q, e fm^2	R_p, fm	$SF(4+3)$	$SF(6+1)$
N	N	0.310	–1.234	–7.286	2.570	1.008	0.781
Y	N	0.438	–1.808	–6.507	2.461	0.993	0.747
N	Y	0.615	–2.173	–6.469	2.381	0.983	0.734
Y	Y	0.587	–2.212	–6.513	2.396	0.981	0.733

T a b l e 3. Correlations between the zero-energy S factor of the reaction ^{4}He(^{3}H,γ)^{7}Li and the energy of the ^{7}Li ground state $E(\frac{3}{2}^-)$, quadrupole moment Q, r.m.s. proton radius R_p, and spectroscopic factor SF for the clusterization ^{4}He+^{3}H and ^{6}Li+n.

Polarization		^{7}Li					
^{3}H	^{6}Li	$S(0)$, keV b	$E\left(\frac{3}{2}^-\right)$, MeV	Q, e fm^2	R_p, fm	$SF(4+3)$	$SF(6+1)$
N	N	0.075	–2.047	–4.045	2.349	1.018	0.784
Y	N	0.085	–2.653	–3.609	2.248	1.002	0.746
N	Y	0.124	–3.033	–3.711	2.173	0.991	0.732
Y	Y	0.108	–3.075	–3.756	2.179	0.990	0.731

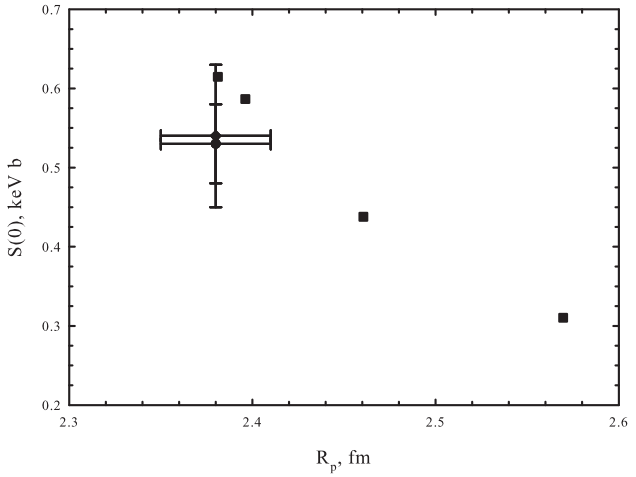

Fig. 6. Zero-energy S factor of the reaction $^4\mathrm{He}\left(^3\mathrm{He},\gamma\right)^7\mathrm{Be}$ as a function of the r.m.s. proton radius

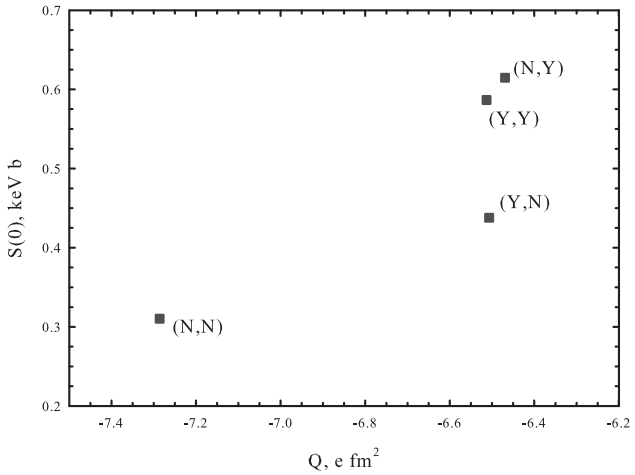

Fig. 7. Astrophysical S factor of the reaction $^4\mathrm{He}\left(^3\mathrm{He},\gamma\right)^7\mathrm{Be}$ as a function of the quadrupole moment of the ground state

both of these values for $S\left(0\right)$. The recommended value of the zero-energy S factor for the reaction $^3\mathrm{H}(\alpha,\gamma)^7\mathrm{Li}$ is $S\left(0\right) = 0.10 \pm 0.02$ keV b [1].

Some types of these correlations have been discussed in the literature. For instance, Kajino [25] investigated the correlations between the S factor for the $^3\mathrm{He}(\alpha,\gamma)^7\mathrm{Be}$ reaction and the r.m.s. proton radius and the quadrupole moment of ^{7}Be calculated within a two-cluster microscopic model with 7 different nucleon-nucleon potentials. He demonstrated the approximate linear correlations between these quantities. In [18], Csótó and Langanke used a two-cluster extended model to calculate the S factor of the reactions $^3\mathrm{He}(\alpha,\gamma)^7\mathrm{Be}$ and $^3\mathrm{H}(\alpha,\gamma)^7\mathrm{Li}$. They considered the correlation between the zero-energy S factor and the quadrupole moment Q. Different values of $S\left(0\right)$ and Q were obtained by varying the parameter u of the Minnesota potential, the Majorana parameter m of the modified Hasegawa–Nagata potential, and the size parameter of interacting clusters.

We have no room to discuss other correlations for the reactions $^3\mathrm{He}(\alpha,\gamma)^7\mathrm{Be}$ and $^3\mathrm{H}(\alpha,\gamma)^7\mathrm{Li}$ and say nothing of the reactions $^6\mathrm{Li}(p,\gamma)^7\mathrm{Be}$ and $^6\mathrm{Li}(n,\gamma)^7\mathrm{Li}$. That is why we summarize the results for ^{7}Be obtained within

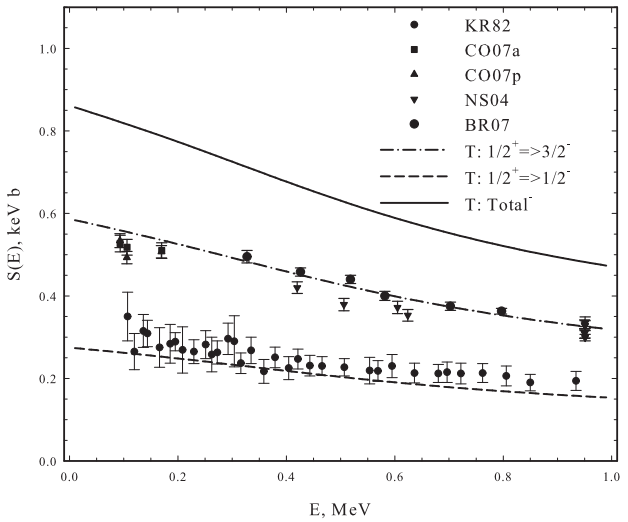

Fig. 8. Theoretical and experimental data for the S factor of the reaction $^3\mathrm{He}(\alpha,\gamma)^7\mathrm{Be}$

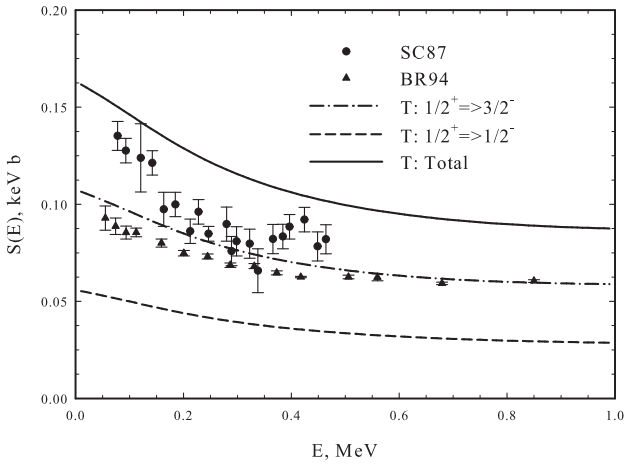

Fig. 9. Astrophysical S factor of the reaction $^3\mathrm{H}(\alpha,\gamma)^7$

the model in Table 2 to demonstrate correlations between the S factor for the reaction $^3\mathrm{He}(\alpha,\gamma)^7\mathrm{Be}$ at zero energy and other quantities related to the ground state. The same quantities for the ^{7}Li ground state and for the S factor of the reaction $^3\mathrm{H}(\alpha,\gamma)^7\mathrm{Li}$ are displayed in Table 3.

One can deduce visually or qualitatively from Figs. 1–3 that the polarization affects very much the astrophysical S factor of the radiative capture reactions. Tables 2 and 3 allow us to quantify these effects. Note that, like in [30, 31], the polarization of ^{6}Li is more pronounced than that of ^{3}He (^{3}H). Indeed, if we compare the S factor at zero energy for the reaction $^3\mathrm{He}(\alpha,\gamma)^7\mathrm{Be}$ with polarization (cases (Y,N) and (N,Y)) and without polarization (case (N,N)), we see that the polarization of ^{6}Li almost double $S(0)$, while the polarization of ^{3}He increases the zero-energy S factor by 1.41 times. For the reaction $^3\mathrm{H}(\alpha,\gamma)^7\mathrm{Li}$, the polarization of ^{6}Li increases $S(0)$ obtained without polarization by 1.65 times, and the polarization of ^{3}H increases it only by 1.13 times.

During the study, we don't aim at reproducing the experimental data for the astrophysical S factor of the reactions $^3\mathrm{He}(\alpha,\gamma)^7\mathrm{Be}$, $^3\mathrm{H}(\alpha,\gamma)^7\mathrm{Li}$, $^6\mathrm{Li}(p,\gamma)^7\mathrm{Be}$ and $^6\mathrm{Li}(n,\gamma)^7\mathrm{Li}$. However, we will compare our theoretical results with available experimental data. For the energy range $0 \le E \le 1$ MeV, we consider only the dipole transition from continuous-spectrum states to the bound states. We also checked that the quadrupole transition gives a small contribution to the S factor in the selected energy range. In Fig. 8, we display theoretical and experimental data for the S factor of the reaction $^3\mathrm{He}(\alpha,\gamma)^7\mathrm{Be}$. Experimental data are taken from KR82 – [45], CO07a and CO07b – [12], NS04 – [17] and BR07 – [11]. One can see that the theoretical results are slightly above the most of experimental data. The S factor of the mirror reaction $^3\mathrm{H}(\alpha,\gamma)^7\mathrm{Li}$ is shown in Fig. 9. Experimental data for this reaction can be found in [46] – SC87 and [47] – BR94. One can see that theoretical results for the reaction $^3\mathrm{H}(\alpha,\gamma)^7\mathrm{Li}$ are much closer to the experimental data than those for the reaction $^3\mathrm{He}(\alpha,\gamma)^7\mathrm{Be}$. By closing this section, we display (Fig. 10) the S factor of $^6\mathrm{Li}(p,\gamma)^7\mathrm{Be}$. Two sets of experimental points for this reaction are used: SW – [48] and PA – [21]. In this case, the theoretical curve is lower than the experimental points.

3. Conclusion

We have developed the three-cluster microscopic model formulated in [30, 31] to study the radiative capture reactions in ^{7}Be and ^{7}Li nuclei. We extended the Hilbert space and included states with different values of the total spin and orbital momentum. The selected three-cluster configurations allowed us to consider the dominant binary channels ^{7}Be and ^{7}Li nuclei. Moreover, the configurations also allowed us to consider the cluster structure of interacting clusters and thus to provide a realistic description of these clusters.

Effects of the cluster polarization have been investigated in detail. It is shown that the cluster polarization affects very much the cross section of the capture reactions $^3\mathrm{He}(\alpha,\gamma)^7\mathrm{Be}$, $^3\mathrm{H}(\alpha,\gamma)^7\mathrm{Li}$, $^6\mathrm{Li}(p,\gamma)^7\mathrm{Be}$

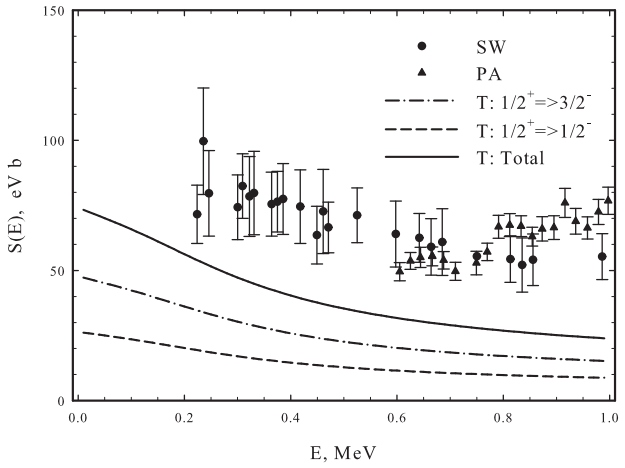

Fig. 10. Comparison of experimental and theoretical data for the S factor of the reaction $^6\mathrm{Li}\,(p,\gamma)^7\mathrm{Be}$

and $^6\mathrm{Li}(n,\gamma)^7\mathrm{Li}$. The polarization of ^{6}Li cluster had a stronger impact on the cross section of the radiative capture reactions, than that of ^{3}He(^{3}H) cluster. This is also true for the reaction $^6\mathrm{Li}(p,\gamma)^7\mathrm{Be}$, where ^{6}Li+$p$ channel is open and dominant, and for the reaction $^3\mathrm{He}(\alpha,\gamma)^7\mathrm{Be}$, where this channel is closed. We have discovered that the reactions $^3\mathrm{He}(\alpha,\gamma)^7\mathrm{Be}$ and $^3\mathrm{H}(\alpha,\gamma)^7\mathrm{Li}$ were much more strongly affected by the cluster polarization, than the reactions $^6\mathrm{Li}(p,\gamma)^7\mathrm{Be}$ and $^6\mathrm{Li}(n,\gamma)^7\mathrm{Li}$.

We have investigated the correlations between the astrophysical S factor of the reactions $^3\mathrm{He}(\alpha,\gamma)^7\mathrm{Be}$ and $^3\mathrm{H}(\alpha,\gamma)^7\mathrm{Li}$ at zero energy $S\,(0)$ and the r.m.s. proton radius and the quadrupole moment of the bound state, as well as the spectroscopic factor for the clusterizations ^{4}He+^{3}He (^{3}H) and ^{6}Li+p (^{6}Li+n). The almost linear dependence of the zero-energy S factor on these quantities is observed in our calculations.

This work was supported in part by the Program of Fundamental Research of the Division of Physics and Astronomy of the National Academy of Sciences of Ukraine.

1. C. Angulo, M. Arnould, M. Rayet *et al.*, Nucl. Phys. A **656**, 3 (1999).
2. E.G. Adelberger, S.M. Austin, J.N. Bahcall *et al.*, Rev. Mod. Phys. **70**, 1265 (1998).
3. J.N. Bahcall and M.H. Pinsonneault, Rev. Mod. Phys. **64**, 885 (1992).
4. G. Wallerstein, I. Iben, jr., P. Parker *et al.*, Rev. Mod. Phys. **69**, 995 (1997).
5. M. Arnould and K. Takahashi, Rep. Prog. Phys. **62**, 393 (1999).
6. H. Costantini, D. Bemmerer, and F. Confortola, Nucl. Phys. A **814**, 144 (2008).
7. A. di Leva, M. de Cesare, D. Schürmann *et al.*, Nucl. Instrum. Meth. Phys. Res., Sect. A **595**, 381 (2008).
8. R.H. Cyburt and B. Davids, Phys. Rev. C **78**, 064614 (2008).
9. A. Di Leva *et al.*, J. Phys. G **35**, 014021 (2008).
10. G. Gyürky, D. Bemmerer, F. Confortola *et al.*, J. Phys. G Nucl. Phys. **35**, 014002 (2008).
11. T.A.D. Brown, C. Bordeanu, K.A. Snover *et al.*, Phys. Rev. C **76**, 055801 (2007).
12. F. Confortola, D. Bemmerer, H. Costantini *et al.*, Phys. Rev. C **75**, 065803 (2007).
13. G. Gyürky, F. Confortola, H. Costantini *et al.*, Phys. Rev. C **75**, 035805 (2007).
14. D. Bemmerer, F. Confortola, H. Costantini *et al.*, Phys. Rev. Lett. **97**, 122502 (2006).
15. H. Costantini, D. Bemmerer, P. Bezzon *et al.*, Eur. J. Phys. A **27**, 177 (2006).
16. B.S. Nara Singh, M. Hass, Y. Nir-El, and G. Haquin, Nucl. Phys. A **758**, 689 (2005).
17. B.S. Singh, M. Hass, Y. Nir-El, and G. Haquin, Phys. Rev. Lett. **93**, 262503 (2004).
18. A. Csótó and K. Langanke, Few-Body Syst. **29**, 121 (2000).
19. Q.K.K. Liu, H. Kanada, and Y.C. Tang, Phys. Rev. C **33**, 1561 (1986).
20. H. Walliser, H. Kanada, and Y.C. Tang, Nucl. Phys. A **419**, 133 (1984).
21. K. Arai, D. Baye, and P. Descouvemont, Nucl. Phys. A **699**, 963 (2002).
22. Q.K.K. Liu, H. Kanada, and Y.C. Tang, Phys. Rev. C **23**, 645 (1981).
23. T. Kajino, G.J. Mathews, and K. Ikeda, Phys. Rev. C **40**, 525 (1989).
24. T. Kajino, H. Toki, K.-I. Kubo, and I. Tanihata, Phys. Lett. B **202**, 475 (1988).
25. T. Kajino, Nucl. Phys. A **460**, 559 (1986).
26. T. Kajino and A. Arima, Phys. Rev. Lett. **52**, 739 (1984).
27. D. Baye and P. Descouvemont, Nucl. Phys. A **407**, 77 (1983).
28. D. Baye and P. Descouvement, Ann. Phys. **165**, 115 (1985).
29. L.L. Chopovsky, Phys. Lett. B **229**, 316 (1989).
30. V.S. Vasilevsky, F. Arickx, J. Broeckhove, and T.P. Kovalenko, Nucl. Phys. **824**, 37 (2009).
31. A.V. Nesterov, V.S. Vasilevsky, and T.P. Kovalenko, Phys. Atom. Nucl. **72**, 1450 (2009).

32. G.F. Filippov, V.S. Vasilevsky, and A.V. Nesterov, Sov. J. Nucl. Phys. **38**, 347 (1983).

33. G.F. Filippov, V.S. Vasilevsky, and L.L. Chopovsky, Sov. J. Part. and Nucl. **16**, 153 (1985).

34. G.F. Filippov, V.S. Vasilevsky, S.P. Kruchinin, and L.L. Chopovsky, Sov. J. Nucl. Phys. **43**, 536 (1986).

35. E.J. Heller and H.A. Yamani, Phys. Rev. A **9**, 1201 (1974).

36. H.A. Yamani and L. Fishman, J. Math. Phys. **16**, 410 (1975).

37. G.F. Filippov and I.P. Okhrimenko, Sov. J. Nucl. Phys. **32**, 480 (1981).

38. G.F. Filippov, Sov. J. Nucl. Phys. **33**, 488 (1981).

39. L. Canton and L.G. Levchuk, Nucl. Phys. A **808**, 192 (2008).

40. D.R. Thompson, M. LeMere, and Y.C. Tang, Nucl. Phys. **A286**, 53 (1977).

41. I. Reichstein and Y.C. Tang, Nucl. Phys. A **158**, 529 1970.

42. O.F. Nemets, V.G.. Neudachin, A.T. Rudchik, Yu.F. Smirnov, and Yu.M. Tchuvil'sky, *Nucleon Clusters in Atomic Nuclei and Many-Nucleon Transfer Reactions* (Naukova Dumka, Kiev, 1988) (in Russian).

43. D.R. Tilley, C.M. Cheves, J.L. Godwin *et al.*, Nucl. Phys. A **708**, 3 (2002).

44. I. Tanihata, H. Hamagaki, O. Hashimoto *et al.*, Phys. Rev. Lett. **55**, 2676 (1985).

45. H. Kräwinkel, H.W. Becker, L. Buchmann *et al.*, Z. Phys. **304**, 307 (1982).

46. U. Schröder, A. Redder, C. Rolfs *et al.*, Phys. Lett. B **192**, 55, (1987).

47. C.R. Brune, R.W. Kavanagh, and C. Rolfs, Phys. Rev. C **50**, 2205 (1994).

48. Z.E. Switkowski, J.C.P. Heggie, D.L. Kennedy *et al.*, Nucl. Phys. A **331**, 50 (1979).

Received 22.01.09

МІКРОСКОПІЧНА МОДЕЛЬ РЕАКЦІЙ РАДІАЦІЙНОГО ЗАХВАТУ З КЛАСТЕРНОЮ ПОЛЯРИЗАЦІЄЮ. ЗАСТОСУВАННЯ ДО ЯДЕР ^{7}Be ТА ^{7}Li

О.В. Нестеров, В.С. Василевський, Т.П. Коваленко

Р е з ю м е

Трикластерну мікроскопічну модель, що була раніше розвинута авторами, застосовано для вивчення впливу кластерної поляризації на протікання реакцій радіаційного захвату $^3\mathrm{He}(\alpha,\gamma)^7\mathrm{Be}$, $^3\mathrm{H}(\alpha,\gamma)^7\mathrm{Li}$, $^6\mathrm{Li}(p,\gamma)^7\mathrm{Be}$ та $^6\mathrm{Li}(n,\gamma)^7\mathrm{Li}$, які є дуже важливими з точки зору астрофізичних застосувань. Головну увагу зосереджено на перерізах (або астрономічних S-факторах) реакцій при малих енергіях. Також детально вивчено кореляції між астрофізичними S-факторами реакцій при нульовій енергії та величинами, які є характеристиками основного стану компаунд-ядра.